JVI Journals.ASM.org

Poliovirus Infection Transiently Increases COPII Vesicle Budding

Meg Trahey,[a] Hyung Suk Oh,[b]* Craig E. Cameron,[b] and Jesse C. Hay[a]

Division of Biological Sciences and Center for Structural and Functional Neuroscience, The University of Montana, Missoula, Montana, USA,[a] and Department of Biochemistry and Molecular Biology, The Pennsylvania State University, University Park, Pennsylvania, USA[b]

Poliovirus (PV) requires membranes of the host cell's secretory pathway to generate replication complexes (RCs) for viral RNA synthesis. Recent work identified the intermediate compartment and the Golgi apparatus as the precursors of the replication "organelles" of PV (N. Y. Hsu et al., Cell 141:799–811, 2010). In this study, we examined the effect of PV on COPII vesicles, the secretory cargo carriers that bud from the endoplasmic reticulum and homotypically fuse to form the intermediate compartment that matures into the Golgi apparatus. We found that infection by PV results in a biphasic change in functional COPII vesicle biogenesis in cells, with an early enhancement and subsequent inhibition. Concomitant with the early increase in COPII vesicle formation, we found an increase in the membrane fraction of Sec16A, a key regulator of COPII vesicle formation. We suggest that the early burst in COPII vesicle formation detected benefits PV by increasing the precursor pool required for the formation of its RCs.

Poliovirus (PV) is a member of the *Picornaviridae* family of small nonenveloped positive-strand RNA viruses. Like other positive-strand viruses, PV replicates within the host cell cytoplasm in membranous replication complexes (RCs) (23). Recent electron tomographic studies by Belov et al. demonstrated that these RCs are convoluted branching structures (3). Data from a number of laboratories suggest that PV coopts the membranes of the early secretory pathway to establish RCs (see reference 1 and references therein). The early secretory pathway transports proteins destined for secretion from the endoplasmic reticulum (ER) to the Golgi apparatus (20, 24). Specifically, cargo-laden COPII vesicles bud from specialized regions of the ER, the transitional ER or ER exit sites (ERES), and fuse homotypically to become an ER/Golgi intermediate compartment (ERGIC) or vesicular tubular cluster (VTC) where protein sorting occurs. Resident ER proteins are returned to the ER via COPI vesicles, and proteins destined for secretion continue on to the Golgi apparatus.

The mechanistic details of COPII vesicle biogenesis have been studied extensively. Vesicle formation is initiated by the interaction of the small GTP-binding protein Sar1 and its nucleotide exchange factor, Sec12, on ER membranes. The exchange of GDP for GTP on Sar1 triggers the membrane insertion of its N-terminal amphipathic alpha helix and the binding of the inner COPII coat subunits (Sec23/24), followed by the outer coat subunits (Sec13/31) (16, 24). The peripheral membrane protein Sec16 is required for this process *in vivo* (6, 10, 18, 31) and enhances this process *in vitro* (28). Sec16 has binding sites for COPII coat proteins (10, 13, 17, 27), and it has been proposed to act as a platform for assembly of the COPII coat (27, 31). Independent of this function, Sec16 has also been shown to be required for the development of ERES in the yeast *Pichia pastoris* (7), in *Drosophila* (19), and in mammalian cells (6, 31).

Mammals have two unique genes with homology to the central conserved domain of yeast Sec16, namely, the Sec16A and Sec16B genes (also known as the Sec16L and -S genes [6]). The Sec16A gene encodes a protein of ~250 kDa, a similar size to that of yeast Sec16, while the Sec16B gene encodes a much smaller protein, of ~117 kDa (6, 18, 31). Based on size and sequence similarity outside the central domain, Sec16A is the likely orthologue of yeast Sec16 (6, 18, 31). Interestingly, recent work by Yonekawa et al. identified a unique cellular role for Sec16B: Sec16B is required for the transport of a specific peroxisome biogenesis factor, Pex16, from the ER to the peroxisome (33).

Rust and colleagues showed that early in PV infection, the viral proteins 2B and 2BC colocalize with COPII coat proteins specifically at ERES (26). These data were used to support the hypothesis that poliovirus coopts COPII vesicles for the formation of RCs. However, recent work by Hsu et al. has shown that PV hijacks later COPII-derived organelles of the ERGIC/Golgi apparatus, generating "remodeled" vesicles devoid of coat proteins but enriched in phosphatidylinositol-4-phosphate lipids (14). This altered lipid composition favors binding of the viral polymerase, facilitating viral RNA synthesis (14). These membrane remodeling events are critically dependent on the poliovirus membrane protein 3A and its association with the host proteins GBF1 and Arf1. Arf1 is a small GTP-binding protein required for assembly of COPI-coated vesicles, and GBF1 is its guanine nucleotide exchange factor (15).

What then is the consequence of the association of PV proteins 2B and 2BC with COPII proteins at ERES? We propose that this association supports an effect of PV infection on COPII vesicle biogenesis. Specifically, we hypothesize that PV infection enhances COPII vesicle formation to enrich the intermediate compartment precursors used for RC formation.

MATERIALS AND METHODS

Cells, viruses, transfection, and infection. NRK (normal rat kidney) and HeLa cells were cultured in complete Dulbecco's modified Eagle's medium with 10% fetal bovine serum, penicillin, and streptomycin. NRK cells expressing the poliovirus receptor (PVR) were generated using the BD RevTet-Off system (BD Biosciences). Briefly, PVR cDNA (a gift from Mattias Gromeier) was cloned into the retroviral vector pLP-RevTRE

Received 9 May 2012 Accepted 20 June 2012
Published ahead of print 27 June 2012
Address correspondence to Jesse C. Hay, jesse.hay@umontana.edu.
* Present address: Hyung Suk Oh, Department of Microbiology and Immunobiology, Harvard Medical School, Boston, Massachusetts, USA.

doi:10.1128/JVI.01159-12

(pLP-RevTRE-PVR). pLP-RevTRE-PVR- and pRevTet-off-containing retrovirus stocks were made as described previously (25). NRK cells coinfected with pLP-RevTRE-PVR- and pRevTet-off-containing retroviruses were cultured in growth medium with 300 μg/ml of hygromycin B and G418. PVR expression was confirmed by Western blotting. The resultant PVR-NRK cells were routinely cultured in growth medium supplemented with 100 μg/ml of hygromycin B and G418. PV type I Mahoney and eGFP-PV (a gift from Raul Andino [8]) stocks were produced in HeLa cells as described previously (25). Briefly, HeLa cells were electroporated with RNA transcribed from linearized plasmid DNA and incubated at 37°C for 2 to 3 days until cytopathic effect became apparent. Infected cells were harvested and virus particles released by three freeze-thaw cycles. For PV infections, cells were seeded in growth medium without hygromycin or G418 and were 90% confluent on the day of infection. Virus was added to cells at room temperature for 30 min with occasional rocking. Cells were washed three times with phosphate-buffered saline (PBS) to remove unadsorbed virus, fresh growth medium was added, and cultures were incubated at 37°C for the indicated times. For budding and fusion experiments using cells expressing the myc-tagged temperature-sensitive mutant G glycoprotein of vesicular stomatitis virus (VSV-G_{ts}-myc), PVR-NRK cells were electroporated with pVSV-G_{ts}-myc DNA. After 3 h of recovery at 37°C, cultures were maintained at the nonpermissive temperature of 40°C overnight. At this temperature, VSV-G_{ts} is unable to fold properly and accumulates in the ER.

Antibodies. The primary antibodies used were mouse anti-myc antibody 9E10 (32), rabbit anti-p24 COPII cargo receptor (4), rabbit anti-sec31A (5), rabbit anti-sec16A (Novus), mouse anti-mannosidase II (Covance), mouse anti-GBF1 (BD Laboratories), goat anti-PGK-1 (Y-12; Santa Cruz Biotechnology, Inc.), rabbit anti-IP3RI (Affinity BioReagents), mouse anti-IP3RIII (BD Laboratories), rabbit anti-calnexin (Assay Designs, Inc.). Species-specific peroxidase-, Cy5-, and Cy3-conjugated secondary antibodies were obtained from Jackson ImmunoResearch, Inc.

Transmission electron microscopy. Mock-infected and PV-infected PVR-NRK cells (multiplicity of infection [MOI], 20) were incubated at 37°C for 8 h, washed with PBS, and fixed with 1% glutaraldehyde for 15 min at room temperature and 60 min on ice. The sample preparation was done essentially as described previously (25). The cell pellet was incubated in 1% reduced osmium tetroxide containing 1% potassium ferricyanide in 0.1 M cacodylate for 60 min, followed by *en bloc* staining with 3% uranyl acetate (UA) in 50% ethanol for 60 min in the dark. After dehydration with ethanol (70 to 95%), embedding was done with 100% Epon (Electron Microscopy Sciences) overnight at 65°C. Thin sections (60- to 90-nm thickness) were prepared and stained with UA-lead citrate. The image was taken using a Jeol JEM 1200 EXII electron microscope in the Electron Microscopy Facility at the Pennsylvania State University.

Budding and fusion reactions. *In vitro* COPII vesicle budding and fusion reactions were performed essentially as described previously (32). PVR-NRK cells were infected with PV as described above for various times, washed, scrape permeabilized in 50 mM HEPES, pH 7.2, 90 mM potassium acetate, and maintained on ice. These semi-intact permeabilized cells, the source of ER, were added to budding reaction mixtures containing rat liver cytosol and an ATP regeneration system. The rat liver cytosol provided necessary soluble COPII and Sar1 proteins. The specificity of the reactions for COPII vesicle formation was tested by performing parallel reactions in the presence of the dominant-negative mutant Sar1 protein (T39N), a GDP-restricted specific inhibitor of COPII vesicle formation (21). Reaction mixtures were incubated on ice (negative control, no budding) or at 32°C (permissive temperature for budding). Budding reactions were centrifuged at 15,000 × *g* to remove donor permeabilized cells, and the supernatants containing released vesicles were centrifuged at 100,000 × *g*. Pellets were dissolved in SDS sample buffer, proteins were resolved by SDS-PAGE, and the amount of vesicles formed was determined by Western blotting using antibodies to the COPII cargo receptor p24 (4). To measure the equivalence of permeabilized cell inputs to the reaction mixtures, blots were stripped and reprobed with antibodies to the ER protein calnexin.

To assess the ability of released vesicles to fuse homotypically, we generated two distinct VSV-G-bearing vesicle populations whose identity and mixing can be followed as diagrammed in Fig. 3. This fusion assay was performed essentially as described previously (32) and exploits the fact that VSV-G trimers exchange subunits only when present in the same membrane. The first vesicle population was generated by using VSV-G_{ts}-myc-transfected PVR-NRK cells. These cells were infected with PV for the indicated times and permeabilized as described above. The second vesicle population was generated from VSV-infected and [^{35}S]methionine-cysteine pulse-labeled cells. These cells were not infected with PV. The released vesicle population from each cell type contains about 1.3% of the total VSV-G protein (32). The two populations were mixed and incubated at 32°C for 1 h. Fusion permits the exchange of VSV-G subunits and generates heterotrimers consisting of a mixture of myc-tagged unlabeled and untagged radioactive VSV-G subunits. Under these conditions, ~2.5% of the released vesicular VSV-G exchanges subunits, generating heterotrimers (32). Fusion reaction mixtures were adjusted to 2% Triton X-100 and centrifuged at 100,000 × *g*. Myc-tagged VSV-G was immunoprecipitated from the 100,000 × *g* supernatants by use of biotinylated 9E10 monoclonal antibody and streptavidin-Sepharose (GE Healthcare). Eluted proteins were resolved by SDS-PAGE, and heterotrimerization was quantified following phosphorimaging to detect coprecipitated radioactive VSV-G.

Immunofluorescence. Cells were cultured in 6-well plates containing poly-L-lysine (0.5 mg/ml)-coated coverslips. Infected cells were washed with PBS and fixed with 4% paraformaldehyde (EM Biosciences) in PBS for 20 min at room temperature. Free aldehydes were quenched with 100 mM glycine in PBS twice for 10 min at room temperature or overnight at 4°C. Cells were permeabilized with IF buffer (PBS supplemented with 0.4% saponin, 2% goat serum, and 1% bovine serum albumin). Antibodies were diluted in IF buffer and incubated with cells at room temperature for 1 h (primary antibodies) or 1/2 h (Cy3- or Cy5-conjugated secondary antibodies). Cultures were washed three times using IF buffer and rocking between antibody incubations. Cells shown in Fig. 4 were visualized using an MHFI Olympus FV1000 laser scanning microscope, and images were processed using Image J. Cells in Fig. 5 were visualized using a Nikon E-800 microscope, and images were collected using an Orca2 digital camera (Hamamatsu, NJ) controlled by OpenLab software (Improvision, United Kingdom).

Cell fractionation. Cells were fractionated essentially as described previously (29). Briefly, cells were trypsinized, pelleted, and resuspended in 50 mM HEPES, pH 7.2, and 90 mM potassium acetate with protease inhibitors on ice. Cells were passed through a 27-gauge needle 20 times, and unbroken cells and nuclei were pelleted at 1,000 × *g* for 10 min. The postnuclear supernatant was separated into cytosolic and membrane fractions by centrifugation at 100,000 × *g*.

Western blotting. For budding assays, proteins were dissolved in SDS sample buffer, boiled for 5 min, resolved in 3 to 20% gradient SDS-polyacrylamide gels, and transferred to nitrocellulose membranes. For fractionation studies, proteins were dissolved in lithium dodecyl sulfate (LDS) sample buffer, heated to 70°C for 10 min, resolved in 3 to 8% Tris-acetate gels (Invitrogen), and transferred to nitrocellulose membranes per the supplier's instructions. Blots were incubated with antibodies diluted in PBS with 5% nonfat milk and 0.05% Tween 20, and bound HRP-conjugated secondary antibodies were detected by enhanced chemiluminescence.

RESULTS AND DISCUSSION

PVR-NRK cells are productively infected by PV. To test for an effect of poliovirus on COPII vesicle formation, we utilized permeabilized NRK cells that have a well-characterized secretory pathway (32). To enable poliovirus infection, NRK cells were engineered to express the human poliovirus receptor. The kinetics of

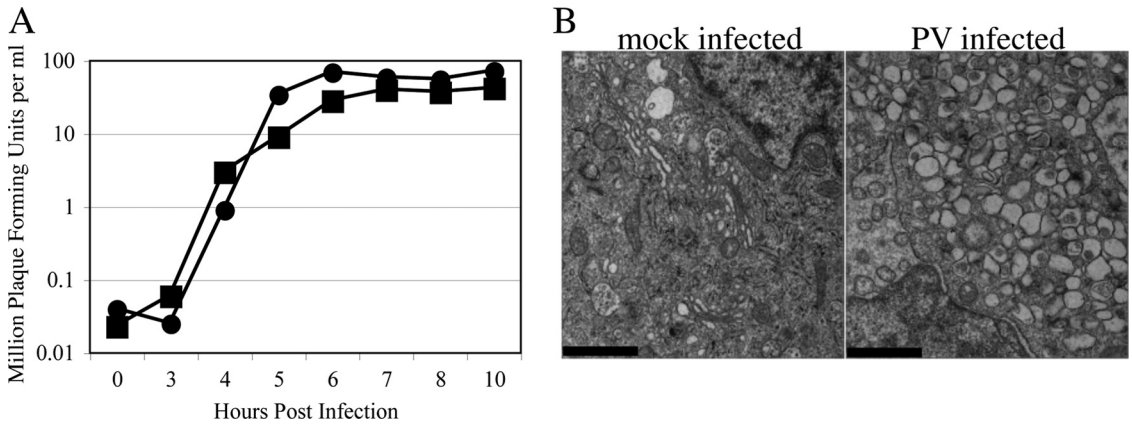

FIG 1 NRK cells stably expressing the poliovirus receptor (PVR-NRK) are productively infected by PV and form membranous RCs. (A) PVR-NRK (squares) or HeLa (circles) cells were infected with PV at an MOI of 10 and incubated at 37°C. At the indicated times postinfection, cells were harvested and lysed by freeze-thawing, and the number of viral PFU in lysates was determined on HeLa cells as previously described (25). (B) PVR-NRK cells were mock infected (left) or infected with PV (right) at an MOI of 20. Cells were fixed at 8 h postinfection and visualized by transmission electron microscopy. Bars = 1 μm. Note the accumulated vesicles in PV-infected cells.

PV production in PVR-NRK cells was compared with that of the well-characterized human host cell line HeLa. As shown in Fig. 1A, PVR-NRK cells were susceptible to infection by PV (type I Mahoney strain) and produced infectious virus with kinetics similar to that of HeLa cells, albeit with a slightly lower yield. In addition, transmission electron microscopy of infected PVR-NRK cells showed robust formation of membranous RCs, as expected (Fig. 1B).

PV infection transiently increases COPII vesicle release from semi-intact PVR-NRK cells. To determine if PV infection altered COPII vesicle biogenesis, we modified a previously described vesicle budding assay (32) to specifically examine endogenous cargo-laden COPII vesicles (Fig. 2A). Infected PVR-NRK cells were scrape permeabilized, and aliquots were added to budding reaction mixtures containing rat liver cytosol and an ATP regeneration system and kept on ice or incubated at 32°C for 30 min. To assess the specificity of the reactions for COPII vesicle formation, parallel reactions were performed in the presence of purified dominant-negative mutant (T39N) Sar1 protein, a GDP-restricted specific inhibitor of COPII vesicle formation (21). Permeabilized cells were pelleted at 15,000 × *g*, the supernatants were collected, and then released vesicles were pelleted at 100,000 × *g*. Pellets were dissolved in SDS sample buffer, and the amount of vesicles formed was determined by Western blotting using antibodies to the COPII membrane cargo protein p24 (4). Relative to the mock-infected cells, there was a 2.3-fold increase in the amount of specific COPII vesicles (total band intensity of 32°C reaction minus the band intensity of the corresponding sar1dn reaction) formed

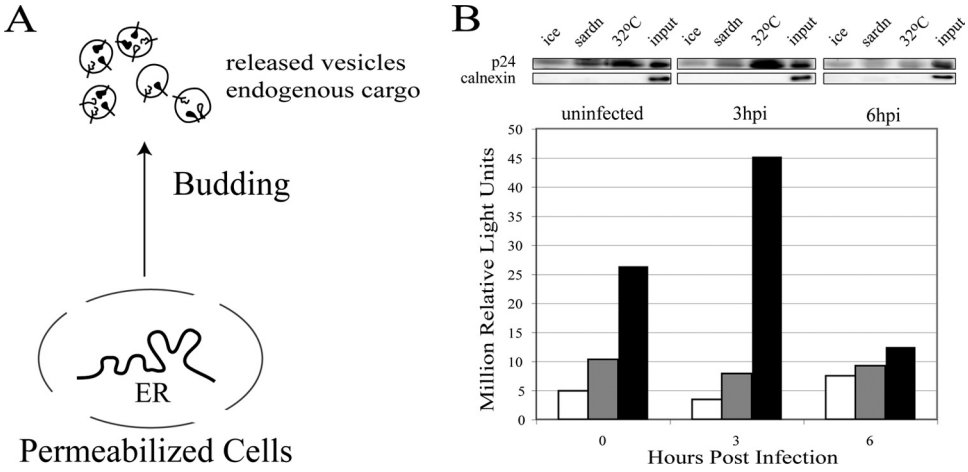

FIG 2 PV infection transiently increases COPII vesicle formation. (A) Schematic of vesicle budding assay measuring endogenous cargo-carrying COPII vesicles. Permeabilized cells are the source of ER for the budding reaction. Soluble proteins required are provided by rat liver cytosol. Released vesicles containing endogenous cargoes are collected by centrifugation at 100,000 × *g* and quantitated by Western blotting using antibodies to the known COPII cargo protein p24. (B) PVR-NRK cells were mock infected or infected with PV at an MOI of 20 for the indicated times. Cells were permeabilized by scraping and added to vesicle budding reaction mixtures on ice (white bars) or at 32°C in the absence (black bars) or presence (gray bars) of T39N Sar1 (sardn), an inhibitor of COPII vesicle formation. Released vesicles and 5% of the input permeabilized cells were analyzed by Western blotting. (Top blot) Results obtained using antibodies to the endogenous cargo receptor protein p24. (Bottom blot) Results obtained using antibodies to the ER chaperone calnexin. Quantitation of the chemiluminescence signals from the p24 series is depicted in the graph.

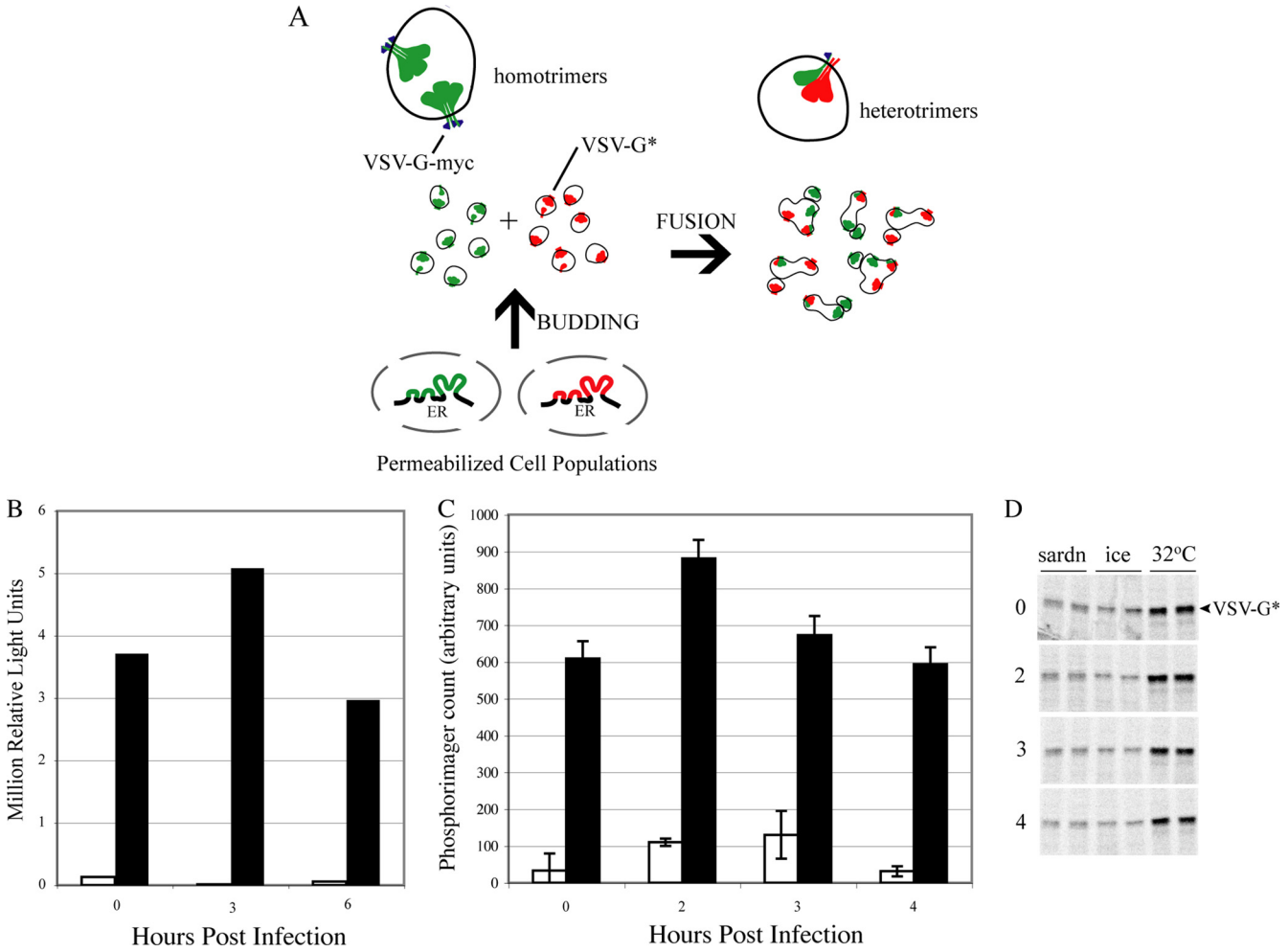

FIG 3 COPII vesicles formed from semi-intact PV-infected cells are capable of homotypic fusion. (A) Schematic of COPII fusion assay. See the text for details. (B) COPII vesicle budding of an ER-accumulated model cargo protein, VSV-G_{ts}-myc, is also increased early in PV infection. PVR-NRK cells were transfected with a plasmid encoding VSV-G_{ts}-myc, and cells were maintained at 40°C to accumulate VSV-G_{ts}-myc in the ER. Transfected cells were infected and permeabilized, and vesicle budding reaction mixtures were kept on ice (white bars) or incubated at 32°C as described in the legend to Fig. 2 (black bars). Released vesicles were quantitated by Western blotting using the mouse monoclonal anti-myc antibody 9E10. (C) COPII vesicles made from PV-infected cells can fuse homotypically. PVR-NRK cells expressing VSV-G_{ts}-myc were mock infected or infected with PV at an MOI of 50. VSV-G_{ts}-myc-containing vesicles were generated as described above, in the absence (black bars) or presence (white bars) of the COPII vesicle inhibitor T39N Sar1. VSV-G_{ts}-myc-containing vesicles were mixed with ^{35}S-labeled untagged VSV-G (VSV-G*)-containing vesicles at 32°C for 1 h. Fused vesicles containing heterotrimers were detected by immunoprecipitating VSV-G_{ts}-myc and quantitating coprecipitated radioactive VSV-G* by phosphorimaging. The increase in MOI used relative to that for panel B resulted in slightly faster replication kinetics, resulting in the peak at 2 h postinfection. The graph depicts quantitation of heterotrimers, with background values (for budding reaction mixtures incubated on ice) subtracted. Error bars represent standard errors of the means (SEM) for duplicate reactions. (D) Phosphorimage of ^{35}S-labeled vesicles quantitated in panel C.

from cells infected with PV for 3 h, followed by a 5-fold decrease in the amount formed by cells infected for 6 h (Fig. 2B, black bars). Vesicle formation was a temperature-dependent process (Fig. 2B, compare 32°C reaction [black bars] with 0°C reaction [white bars]) and was significantly inhibited in the presence of the dominant-negative mutant Sar1 protein, indicating that these were COPII vesicles (Fig. 2B, gray bars). Similar results were obtained when the vesicles were probed with an antibody to another endogenous COPII vesicle cargo, the SNARE protein rbet1 (data not shown). The decrease in vesicle formation at late times was expected, as it has been shown that protein secretion is completely inhibited at this point in infection (9). However, the enhancement of COPII formation from the ER of cells early in the infection time course was surprising.

Vesicle fusion assay. To determine whether the COPII vesicles formed in PV-infected cells are functional, i.e., capable of homotypic fusion to generate VTCs, we employed a vesicle fusion assay (32) (Fig. 3A). This assay utilizes vesicles released from two populations of cells expressing unique versions of a model cargo protein, the temperature-sensitive trimeric G protein of the vesicular stomatitis virus (VSV-G_{ts}). One cell population expresses a transfected myc-tagged version of VSV-G_{ts} and the other cell population expresses an untagged but [^{35}S]methionine-cysteine-labeled version driven by VSV infection. These cell populations are used in separate budding reactions to generate COPII vesicles carrying distinguishable VSV-G trimers. The released vesicles are then mixed to allow fusion to occur. Upon fusion, the VSV-G trimers exchange subunits, generating heterotrimers containing a mix-

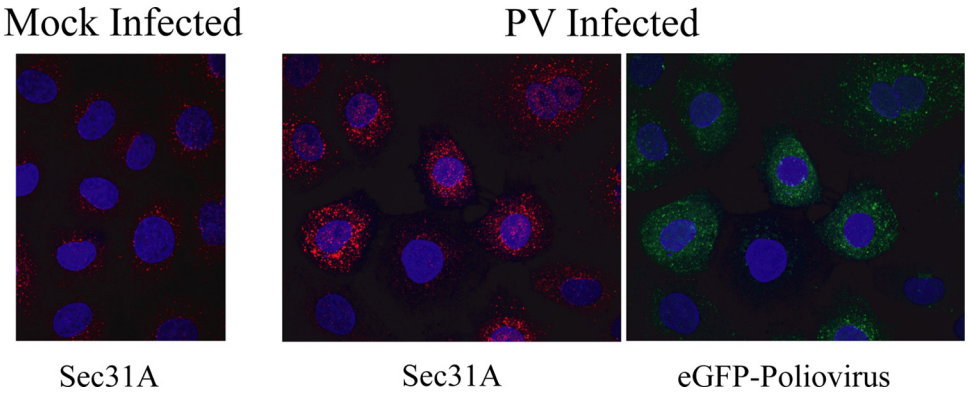

FIG 4 Changes in Sec31A-labeled ERES early in PV infection. PVR-NRK cells were mock infected (left) or infected with eGFP-PV at an MOI of 10 for 2 h (middle and right panels), fixed with 4% paraformaldehyde, permeabilized with 0.4% saponin, and labeled with rabbit anti-Sec31A followed by anti-rabbit Cy3. Nuclei were visualized using DAPI (4′,6-diamidino-2-phenylindole). Images are *z* projections collected using an MHFI Olympus FV1000 laser scanning microscope.

ture of myc-tagged cold and untagged radioactive VSV-G subunits. The trimers are immunoprecipitated using an antibody to the myc tag, and the amount of radioactive VSV-G coprecipitated is quantified by SDS-PAGE and phosphorimaging. In our adaptation of this assay, the cell population expressing the transfected myc-tagged VSV-G is mock infected or infected with PV for various times. Vesicles generated from these cells, of unknown fusogenicity, are then mixed with an aliquot of fusion-competent "test vesicles" (identical in every incubation) derived from the metabolically labeled VSV-infected cells. We have found that VSV infection of the partner cell population, rather than recombinant expression, is required to generate reliably detectable levels of [^{35}S]VSV-G counts in the fused vesicles (32). We cannot formally exclude the possibility that effects of PV infection could be modulated by VSV infection of cells producing the [^{35}S]VSV-G-labeled vesicle.

COPII vesicles formed from semi-intact PV-infected cells are functional for homotypic fusion. PVR-NRK cells were electroporated with a plasmid encoding myc-tagged VSV-G (VSV-G_{ts}-myc) and maintained at a restrictive temperature (40°C) to allow the protein to accumulate within the ER. The transfected cells were infected with PV for the indicated times as described for Fig. 2B, except that the temperature was maintained at 40°C. Permeabilized cells from these cultures were used in budding reaction mixtures at 32°C (a permissive temperature), and the movement of VSV-G_{ts} into COPII vesicles was detected by Western blotting using the mouse monoclonal anti-myc antibody 9E10 (32). We again detected an increase in vesicles formed from cells early in infection followed by a decrease late in infection, confirming that the alteration in COPII biogenesis seen with endogenous cargo (Fig. 2B) is also found using overexpressed exogenous cargo (Fig. 3B).

To assess the fusion competence of these vesicles formed from PV-infected cells, vesicles from reactions similar to those whose results are shown in Fig. 3B were mixed with equal amounts of vesicles prepared from VSV-infected and [^{35}S]methionine-cysteine pulse-labeled cells. The formation of VSV-G heterotrimers was quantified following anti-myc immunoprecipitation, SDS-PAGE, and phosphorimaging to detect radioactive VSV-G. As shown in Fig. 3C, vesicles formed from cells infected with PV for 2, 3, or 4 h retained the ability to fuse homotypically. The increase in the fusion signal at 2 hpi is consistent with the enhanced budding previously observed (Fig. 2B and 3B). Collectively, the data suggest that PV infection induces an early (2 to 3 hpi) enhancement in the budding of functional COPII vesicles, followed by a subsequent inhibition by 6 hpi.

Changes in Sec31A labeling of ERES parallel observed changes in COPII budding. The increase in COPII vesicle formation we observed early in PV infection could be due to a change in ERES, either quantitatively or qualitatively. To assess this possibility, we labeled infected cells with antibodies to the COPII coat protein Sec31A, an established marker for ERES (11). We detected a notable change in Sec31A staining at 2 h postinfection with PV, with an increase in the brightness of ERES (Fig. 4). The images in Fig. 4 are representative of findings from four independent experiments. Counting of total puncta/cell by use of Open Lab software did not show a significant increase in the number of ERES, consistent with the findings of Hsu et al. (14). We did, however, find that the percentage of "large ERES" (>10 pixels) per cell was modestly higher (1.3-fold) for the infected than for the mock-infected population. These data suggested to us that if a change in ERES was responsible for the increased COPII budding, then the change was an increase in size or perhaps a qualitative change in the ERES, such as an increase in the density of Sec31A on the membrane.

Increased levels of membrane-associated Sec16A indicate functional changes in ERES early in PV infection. The COPII vesicle budding reactions used to create Fig. 2 utilized only the membranes from the infected cells; soluble factors were provided by added rat liver cytosol. Therefore, it is presumably a change in a membrane-associated protein that is responsible for the increase in vesicle budding observed. A prime candidate is Sec16A, a peripheral membrane protein that is hypothesized to act as a platform for COPII assembly at ERES (27, 31), is required for ERES formation (6, 7, 19, 31), and stimulates COPII vesicle budding *in vitro* in *Saccharomyces cerevisiae* (28). Perhaps even more relevant is recent work from several laboratories pointing to a regulatory role for Sec16A in COPII vesicle formation. The Hauri group has shown that Sec16 is required for cells to adapt to changes in ER cargo load and that Sec16 can be phosphorylated via the mitogen-activated protein kinase (MAPK) signaling pathway to increase the number of ERES per cell (11, 12). Zacharogianni et al. have shown that in response to amino acid starvation, Sec16 is phosphorylated on its C terminus and loses its association with ER membranes, resulting in a loss of ERES (34). Most recently, a

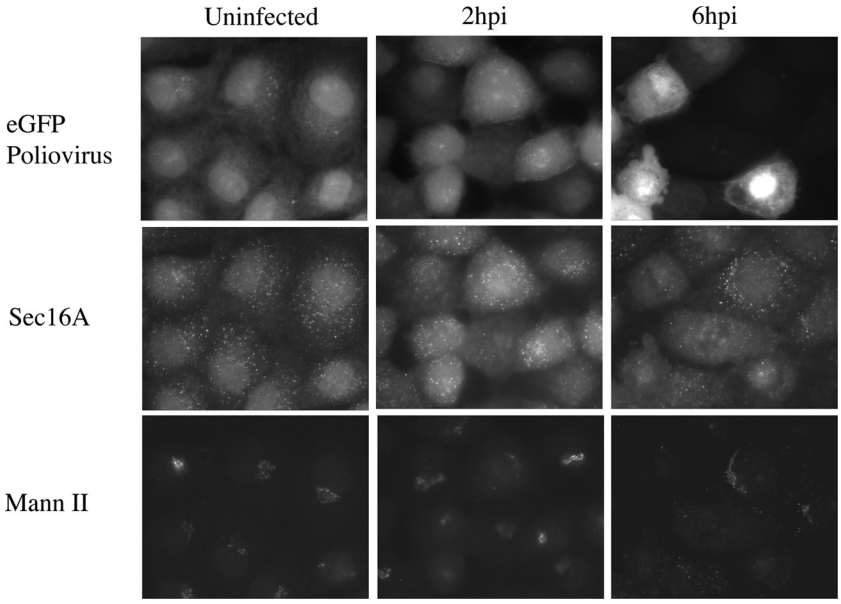

FIG 5 Increase in Sec16A detected by indirect immunofluorescence early in PV infection. PVR-NRK cells were mock infected or infected with eGFP-PV at an MOI of 10 for 2 or 6 h. Cells were fixed with 4% paraformaldehyde, permeabilized with 0.4% saponin, labeled with rabbit anti-Sec16A followed by anti-rabbit Cy3, and colabeled with mouse anti-mannosidase II (Mann II) followed by anti-mouse Cy5. Images were collected using a Nikon E-800 wide-field microscope and an Orca2 digital camera.

paper by Kung et al. showed that Sec16 without an N-terminal domain can inhibit the GAP activity of Sec23/Sec31 toward Sar1p, altering the number and size of ERES (22). These studies suggest that changes in Sec16A could lead to the increase in COPII vesicle formation we detect early in PV infection.

To probe for any changes in Sec16A upon infection, we labeled PVR-NRK cells infected with eGFP-PV with antibodies to Sec16A and the Golgi resident mannosidase II (Fig. 5). There were distinct changes in Sec16A labeling by 2 h postinfection, with a dramatic increase in diffuse cytosolic labeling as well as an increase in the intensity of puncta representing ERES. This result is consistent with the changes we detected in Sec31A labeling in Fig. 4. These changes disappeared later in infection (Fig. 5, 6hpi). The mannosidase II staining of the Golgi apparatus was used as an independent indicator of the progression of infection. As evident in the bottom panels of Fig. 5, the Golgi apparatuses of cells infected for 2 h were mostly intact but fully dispersed by 6 h, consistent with the eventual shutoff of secretion (9).

If the increase in Sec16A labeling of ERES detected by immunofluorescence represents an increase in the membrane-bound fraction of Sec16A, this should be detectable by Western blotting of fractionated cells. At various times post-PV infection, cells were fractionated as described by Szul et al. (29). Cells were triturated through a 27-gauge needle and the postnuclear supernatant separated into membrane and cytosol fractions by centrifugation at 100,000 × *g*. Proteins were resolved in 3 to 8% Tris-acetate gels and transferred to nitrocellulose membranes for Western blotting. The effectiveness of the fractionation method was validated using antibodies to the transmembrane protein IP3 receptor type I (IP3RI) and soluble PGK1, as shown in the bottom panels of Fig. 6A. By 2 h after infection with PV, the amount of Sec16 was increased in both membrane and cytosolic pools, consistent with the changes detected by immunofluorescence (Fig. 6A, top panel, and B [quantitation]). This PV-induced increase in the membrane fraction of Sec16A was, on average, 2-fold (four independent experiments). Also consistent with the immunofluorescence data, the increase in cytosolic Sec16A was short-lived. When blots were probed with antibodies to the COPII coat protein Sec31A, we detected a transient increase in both membrane and cytosolic pools of a Sec31A doublet (30), in agreement with the immunofluorescence data from Fig. 4. PV infection has been shown to increase the membrane association of GBF1, a guanine nucleotide exchange factor for Arf1, a change that occurs early in infection and is critical to the establishment of RCs (1, 2). In the second panel of Fig. 6A (quantitation is shown in Fig. 6B), we see a 1.7-fold increase in the amount of membrane-bound GBF1 by 2 h postinfection, indicating that the timing of events is similar, with membrane-associated Sec16A increasing in parallel with GBF1. These data suggest that concomitant with the increase in COPII vesicle budding from ERES early in PV infection, there is a stabilization and/or induction of Sec16A protein resulting in an increase in the amount of membrane-associated Sec16A. In order to confirm the increase in total Sec16A early in infection, PV- and mock-infected total cell extracts were directly compared at 3 hpi by Western blotting using antibodies to Sec16A and IP3RIII (as a loading control). As shown in Fig. 6C, PV infection resulted in a 1.8-fold increase in the amount of Sec16A, consistent with the cell fractionation data. We propose that the increase in the functionally relevant membrane fraction of Sec16A is responsible, at least in part, for the increase in COPII vesicle formation observed.

The increase in COPII vesicles observed early in PV infection of cells may provide a benefit for either the host cell or the virus. For the host, this increase in vesicles may be the last opportunity to present viral antigens by major histocompatibility complex (MHC) class I molecules before host translation and secretion are completely inhibited. Clearly, this would be a race between the virus and the cell, as work from the Kirkegaard group has demonstrated that at similar times postinfection in HeLa cells, there is

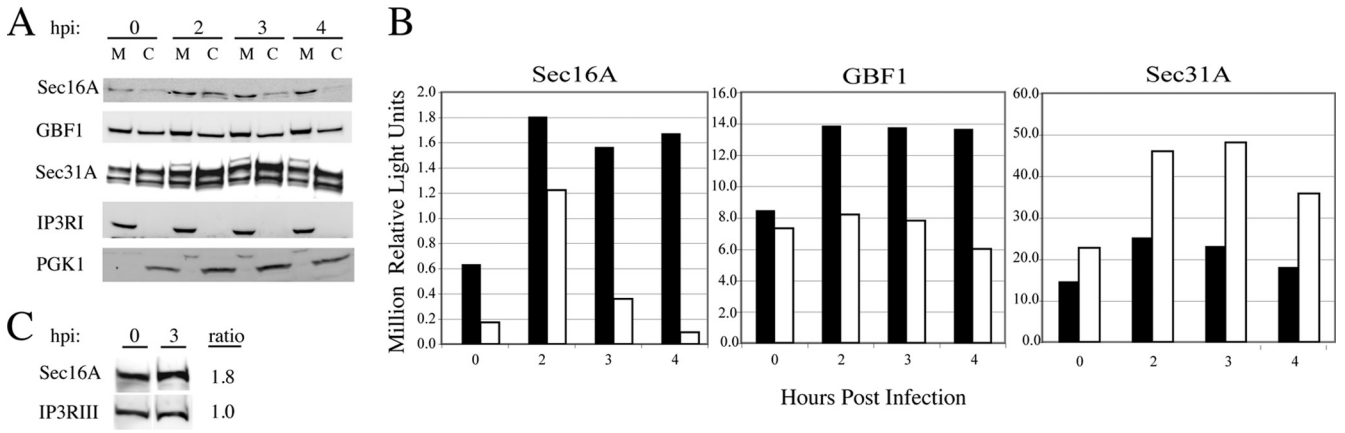

FIG 6 Increases in Sec16A levels in membrane and cytosolic fractions early in PV infection. (A) PVR-NRK cells were mock infected or infected with PV at an MOI of 50 for 2, 3, or 4 h. Membrane (M) and cytosolic (C) fractions were resolved in 3 to 8% Tris-acetate gels and analyzed by Western blotting using rabbit polyclonal anti-Sec16A, mouse monoclonal anti-GBF1, rabbit polyclonal anti-Sec31A, rabbit polyclonal anti-IP3RI, and goat polyclonal anti-PGK1 followed by species-specific peroxidase-conjugated secondary antibodies. (B) Graph of chemiluminescence signals for membrane (black bars) and cytosolic (white bars) fractions from Sec16A, GBF1, and Sec31A blots quantitated using ImageGauge software (Fujifilm). (C) PVR-NRK cells were mock infected or infected with PV at an MOI of 50 for 3 h. Cells were trypsinized and counted, equal cell numbers were lysed in 0.25% CHAPS with protease inhibitors, and the protein concentration in cleared lysates was determined by the Bradford method. Lysates (100 μg) were resolved in Tris-acetate gels, and Western analysis was performed as described for panel A, using rabbit polyclonal anti-Sec16A and mouse monoclonal anti-IP3RIII antibodies. Signals were quantitated, and the ratios for infected (3 hpi) to mock-infected (0 hpi) cells are displayed.

significant (~50%) inhibition of protein secretion (9). If, on the other hand, the enhanced vesicle formation benefits the virus, one would expect that blockade of COPII vesicle biogenesis would inhibit viral replication, and this is indeed the case. Replication of a PV replicon is reduced 50% by the expression of a dominant-negative mutant of Sar1 (14).

The nature of the early secretory pathway is fundamentally interconnected—an increase in COPII vesicles leads to an increase in VTCs, essentially "feeding forward" into the pathway for RC formation. We propose that a transient burst in COPII vesicles benefits the virus by increasing the amount of precursor membranes for RC formation and that this change is mediated by the observed increase in membrane-bound Sec16A. The mechanistic basis for this change is under investigation.

ACKNOWLEDGMENTS

We thank Jack Nunberg for a critical reading of the manuscript, Lou Herritt and the MHFI Core at the University of Montana (supported by National Center for Research Resources award P20RR017670), and Greg Ning and staff of the electron microscope facility at the Pennsylvania State University.

This work was supported by grants from the National Institutes of Health (GM59378 [M.T. and J.C.H.] and AI053531 [H.S.O. and C.E.C.]).

REFERENCES

1. **Belov GA, Ehrenfeld E.** 2007. Involvement of cellular membrane traffic proteins in poliovirus replication. Cell Cycle **6**:36–38.
2. **Belov GA, et al.** 2007. Hijacking components of the cellular secretory pathway for replication of poliovirus RNA. J. Virol. **81**:558–567.
3. **Belov GA, et al.** 2012. Complex dynamic development of poliovirus membranous replication complexes. J. Virol. **86**:302–312.
4. **Bentley M, et al.** 2006. SNARE status regulates tether recruitment and function in homotypic COPII vesicle fusion. J. Biol. Chem. **281**:38825–38833.
5. **Bentley M, et al.** 2010. Vesicular calcium regulates coat retention, fusogenicity, and size of pre-Golgi intermediates. Mol. Biol. Cell **21**:1033–1046.
6. **Bhattacharyya D, Glick BS.** 2007. Two mammalian Sec16 homologues have nonredundant functions in endoplasmic reticulum (ER) export and transitional ER organization. Mol. Biol. Cell **18**:839–849.
7. **Connerly PL, et al.** 2005. Sec16 is a determinant of transitional ER organization. Curr. Biol. **15**:1439–1447.
8. **Crotty S, Hix L, Sigal LJ, Andino R.** 2002. Poliovirus pathogenesis in a new poliovirus receptor transgenic mouse model: age-dependent paralysis and a mucosal route of infection. J. Gen. Virol. **83**:1707–1720.
9. **Doedens JR, Kirkegaard K.** 1995. Inhibition of cellular protein secretion by poliovirus proteins 2B and 3A. EMBO J. **14**:894–907.
10. **Espenshade P, Gimeno RE, Holzmacher E, Teung P, Kaiser CA.** 1995. Yeast SEC16 gene encodes a multidomain vesicle coat protein that interacts with Sec23p. J. Cell Biol. **131**:311–324.
11. **Farhan H, Weiss M, Tani K, Kaufman RJ, Hauri HP.** 2008. Adaptation of endoplasmic reticulum exit sites to acute and chronic increases in cargo load. EMBO J. **27**:2043–2054.
12. **Farhan H, et al.** 2010. MAPK signaling to the early secretory pathway revealed by kinase/phosphatase functional screening. J. Cell Biol. **189**:997–1011.
13. **Gimeno RE, Espenshade P, Kaiser CA.** 1996. COPII coat subunit interactions: Sec24p and Sec23p bind to adjacent regions of Sec16p. Mol. Biol. Cell **7**:1815–1823.
14. **Hsu NY, et al.** 2010. Viral reorganization of the secretory pathway generates distinct organelles for RNA replication. Cell **141**:799–811.
15. **Hsu VW, Yang JS.** 2009. Mechanisms of COPI vesicle formation. FEBS Lett. **583**:3758–3763.
16. **Hughes H, Stephens DJ.** 2008. Assembly, organization, and function of the COPII coat. Histochem. Cell Biol. **129**:129–151.
17. **Hughes H, et al.** 2009. Organisation of human ER-exit sites: requirements for the localisation of Sec16 to transitional ER. J. Cell Sci. **122**:2924–2934.
18. **Iinuma T, et al.** 2007. Mammalian Sec16/p250 plays a role in membrane traffic from the endoplasmic reticulum. J. Biol. Chem. **282**:17632–17639.
19. **Ivan V, et al.** 2008. Drosophila Sec16 mediates the biogenesis of tER sites upstream of Sar1 through an arginine-rich motif. Mol. Biol. Cell **19**:4352–4365.
20. **Klumperman J.** 2000. Transport between ER and Golgi. Curr. Opin. Cell Biol. **12**:445–449.
21. **Kuge O, et al.** 1994. Sar1 promotes vesicle budding from the endoplasmic reticulum but not Golgi compartments. J. Cell Biol. **125**:51–65.
22. **Kung LF, et al.** 2011. Sec24p and Sec16p cooperate to regulate the GTP cycle of the COPII coat. EMBO J. **31**:1014–1027.
23. **Miller S, Krijnse-Locker J.** 2008. Modification of intracellular membrane structures for virus replication. Nat. Rev. Microbiol. **6**:363–374.

24. **Miller EA, Barlowe C.** 2010. Regulation of coat assembly—sorting things out at the ER. Curr. Opin. Cell Biol. **22**:447–453.
25. **Oh HS, Pathak HB, Goodfellow IG, Arnold JJ, Cameron CE.** 2009. Insight into poliovirus genome replication and encapsidation obtained from studies of 3B-3C cleavage site mutants. J. Virol. **83**:9370–9387.
26. **Rust RC, et al.** 2001. Cellular COPII proteins are involved in production of the vesicles that form the poliovirus replication complex. J. Virol. **75**: 9808–9818.
27. **Shaywitz DA, Espenshade PJ, Gimeno RE, Kaiser CA.** 1997. COPII subunit interactions in the assembly of the vesicle coat. J. Biol. Chem. **272**:25413–25416.
28. **Supek F, Madden DT, Hamamoto S, Orci L, Schekman R.** 2002. Sec16p potentiates the action of COPII proteins to bud transport vesicles. J. Cell Biol. **158**:1029–1038.
29. **Szul T, et al.** 2005. Dissection of membrane dynamics of the ARF-guanine nucleotide exchange factor GBF1. Traffic **6**:374–385.
30. **Tang BL, et al.** 2000. Mammalian homologues of yeast sec31p. An ubiquitously expressed form is localized to endoplasmic reticulum (ER) exit sites and is essential for ER-Golgi transport. J. Biol. Chem. **275**:13597–13604.
31. **Watson P, Townley AK, Koka P, Palmer KJ, Stephens DJ.** 2006. Sec16 defines endoplasmic reticulum exit sites and is required for secretory cargo export in mammalian cells. Traffic **7**:1678–1687.
32. **Xu D, Hay JC.** 2004. Reconstitution of COPII vesicle fusion to generate a pre-Golgi intermediate compartment. J. Cell Biol. **167**:997–1003.
33. **Yonekawa S, et al.** 2011. Sec16B is involved in the endoplasmic reticulum export of the peroxisomal membrane biogenesis factor peroxin 16 (Pex16) in mammalian cells. Proc. Natl. Acad. Sci. U. S. A. **108**:12746–12751.
34. **Zacharogianni M, et al.** 2011. ERK7 is a negative regulator of protein secretion in response to amino-acid starvation by modulating Sec16 membrane association. EMBO J. **30**:3684–3700.